

# Lawrence Berkeley National Laboratory

## Lawrence Berkeley National Laboratory

### Title

Methane hydrate formation and dissociation in a partially saturated sand

### Permalink

<https://escholarship.org/uc/item/8028746b>

### Authors

Kneafsey, Timothy J.  
Tomutsa, Liviu  
Taylor, Charles E.  
et al.

### Publication Date

2004-11-24

## Methane hydrate formation and dissociation in a partially saturated sand

Timothy J. Kneafsey<sup>1</sup>, Liviu Tomutsa<sup>1</sup>, Charles E. Taylor<sup>2</sup>, Arvind Gupta<sup>3</sup>, George Moridis<sup>1</sup>, Barry Freifeld<sup>1</sup>, and Yongkoo Seol<sup>1</sup>

<sup>1</sup> Lawrence Berkeley National Laboratory, 1 Cyclotron Rd, Berkeley, CA 94720

<sup>2</sup> National Energy Technology Laboratory, 626 Cochran Mill Rd, Pittsburgh, PA 15236-0940

<sup>3</sup> Colorado School of Mines, PO Box 4028, Golden, CO 80401-1887

### Introduction

To predict the behavior of hydrate-bearing sediments and the economic extractability of natural gas from reservoirs containing gas hydrates, we need reservoir simulators that properly represent the processes that occur, as well as accurate parameters. Several codes are available<sup>1-3</sup> that represent some or all of the expected processes, and values for some parameters are available. Where values are unavailable, modelers have used estimation techniques to help with their predictions. Although some of these techniques are well respected, measurements are needed in many cases to verify the parameters.

We have performed a series of experiments in a partially water saturated silica sand sample. The series included methane hydrate formation, and dissociation by both thermal stimulation and depressurization. The sample was 7.6 cm in diameter and 25 cm in length. In addition to measuring the system pressure and temperatures at four locations in the sample, we measured local density within the sample using x-ray computed tomography. Our goals in performing the experiment were to gather information for estimating thermal properties of the medium and to examine nonequilibrium processes.

### Experimental

We packed a 7.6 cm inside diameter aluminum pressure vessel with moist F110 sand (U.S. Silica, Berkeley Springs WV, with grain sizes ranging from ~50 to 300 microns) to an average porosity of 0.356 and an average water saturation of 0.575. Four type-T thermocouples (Omega Engineering, Stamford, CT) were contained within the sand (**Figure 1**) near the midplane. Three of the four thermocouples were placed near the vessel wall but well within the sand, while the fourth was placed near the sample center. Three thermocouples were placed in the vertical plane to capture effects expected from a gravity-influenced saturation gradient. The vessel was placed in a jacket through which fluid from a temperature controller was flowed. Pressure was measured using a pressure transducer (Rosemount, Chanhassen, MN) connected to the gas inlet line.

A series of tests was performed on the sample including

1. Hydrate formation
2. Thermal test with hydrate present and thermal stimulation resulting in dissociation
3. Second hydrate formation

4. Dissociation by depressurization coupled with thermal stimulation

The pressure-temperature pathway for these tests is shown in **Figure 2**.

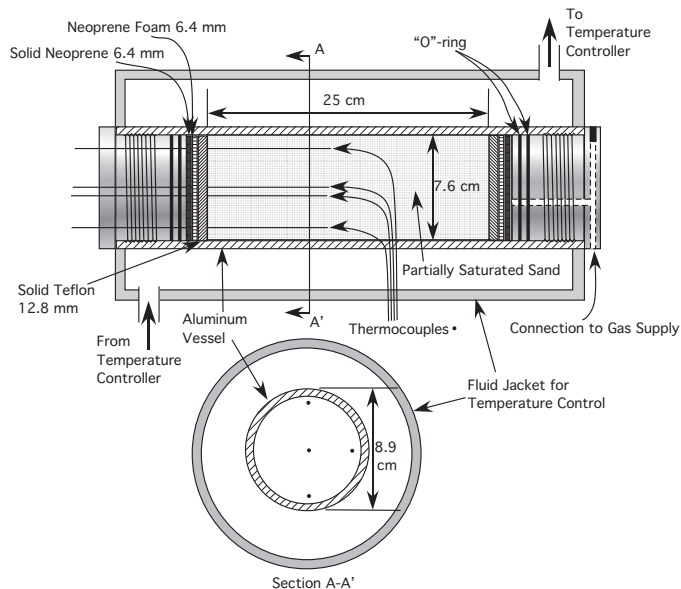


**Figure 1.** Experiment system schematic

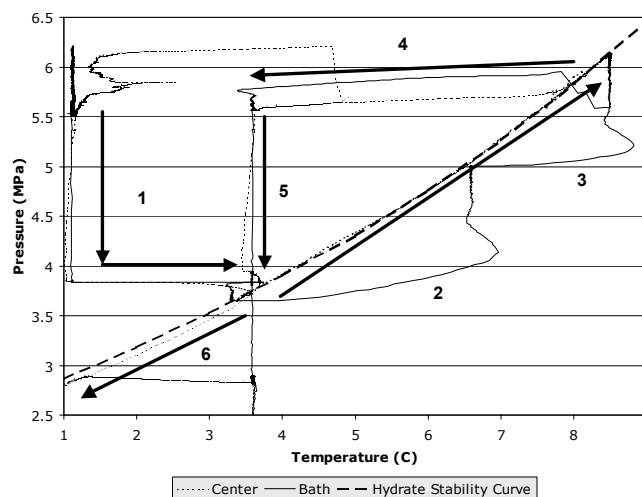


**Figure 2.** Experiment path: (1) hydrate formation, (2) and (3) thermal-stimulation-induced dissociation, (4) second hydrate formation, (5) depressurization prior to dissociation, and (6) dissociation by depressurization/thermal stimulation.

**Hydrate Formation.** Methane hydrate was formed by introducing methane at 6.2 MPa into the sample while it was maintained at 1.3°C. Gas introduction caused the sample temperature to increase by as much as 3.5°C, as a result of gas compression and exothermic hydrate formation. Hydrate formation was sporadic with the rate of hydrate formation

being high initially, then decreasing, and then increasing sharply after about 6 hours, after which the rate again declined. When the rate became small after about 20 hours, hydrate formation was assumed to be complete. From pressure and temperature measurements, we calculated hydrate conversion to be 63%. In contrast, Waite et al. 2004<sup>4</sup> had conversion >90% with formation taking place over several hundred hours. Comparing Images 1 and 2 in **Figure 3** shows a density increase through the sample. Relative density changes were greater where the porosity was initially slightly higher, indicating initial or preferential hydrate formation in these locations.

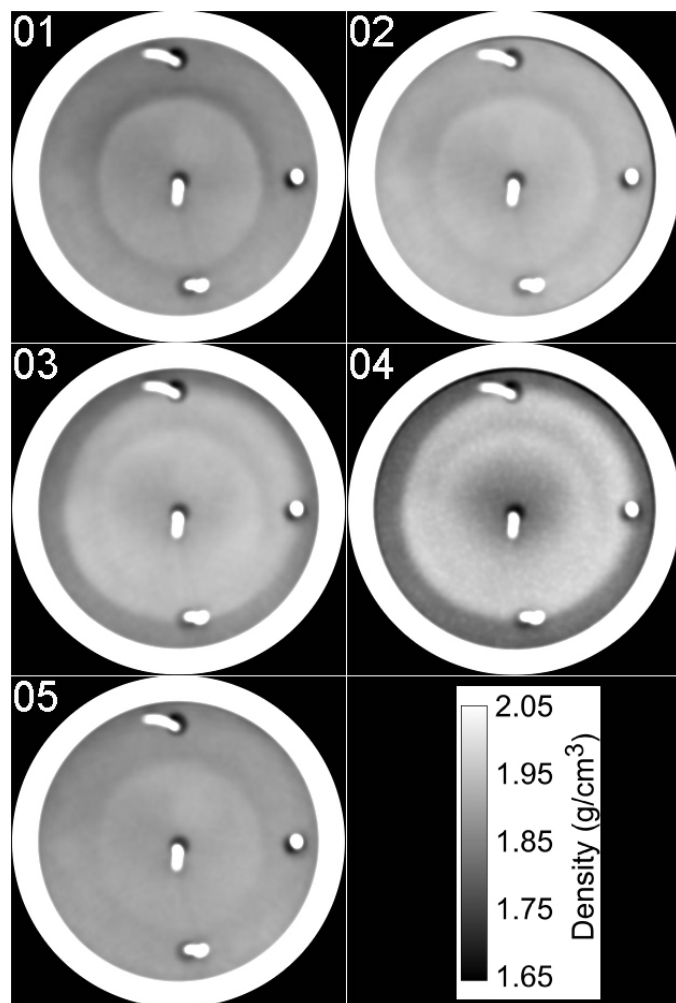


**Figure 3.** Sample density averaged over the length of the sample: (1) initial, (2) after hydrate formation, (3) after thermal stimulation steps, (4) after second hydrate formation, (5) after final dissociation.

**Thermal Test with Hydrate Present and Thermal Stimulation Resulting in Dissociation.** The pressure was reduced to bring the system closer to equilibrium, after which the temperature of the fluid in the jacket was increased in three sharp steps. The system was allowed to vent into a small vessel, and the change in pressure was used to quantify

hydrate dissociated. The first step was within the hydrate stability zone, and the second and third steps induced dissociation. This first step was performed to enable estimation of thermal conductivity of the sand/hydrate/water system. The results were complicated, however, by a sudden surge in hydrate formation despite the reduced driving force caused by depressurization. This was likely caused by dissolved gas in isolated water pockets exsolving on pressure reduction creating a connected pathway to the free gas phase.

As dissociation occurred near the vessel wall, the pressure increased. Because the permeability of the system is relatively high, the pressure increase occurred within the entire vessel, and no pressure gradients were expected. Interestingly, because the pressure increase was sensed very rapidly throughout the vessel and the temperature pulse was delayed because of the thermal conductivity of the system, conditions in the vessel center tended to become more stable for the hydrate, rather than less so.

The change in average density from before thermal stimulation to after thermal stimulation can be seen by comparing Images 2 and 3 in **Figure 3**. Density decreases in a ring near the vessel wall and increases slightly inside the ring. The magnitude of the density decrease near the vessel wall indicates that not only did dissociation occur, but the water saturation in this region decreased.

**Second Hydrate Formation.** Following thermal stimulation, the system was returned to conditions of hydrate stability (6 MPa, 3.6°C) to allow hydrate to form again. This hydrate formation step only required a few hours and resulted in slightly greater hydrate abundance than prior to thermal stimulation. Hydrate did not form in the precise locations where dissociation occurred, but occurred preferentially in a broad ring around the center. Density actually decreased slightly where thermal dissociation had occurred, and also in the sample center (**Figure 3**, Image 4).

**Dissociation by Depressurization Coupled with Thermal Stimulation.** Following the second hydrate formation and prior to the final dissociation, the system was rapidly depressurized to just above the equilibrium point. This depressurization induced additional hydrate formation, resulting in a slight temperature increase and continued slight pressure decline. Upon approaching the equilibrium point, the pressure was reduced over several minutes from 3.8 MPa to about 2.83 MPa, where it remained relatively constant for the duration of the experiment. Upon this depressurization, the temperature in the sample dropped to as low as 1°C as a result of gas expansion and hydrate dissociation. Fluid in the jacket was maintained at 3.6°C, providing heat for thermal stimulation. The temperatures in the three outer thermocouples began to rise towards the jacket temperature, but the temperature in the sample center remained at about 1.3°C for over an hour as dissociation occurred. Conditions in the sample center were clearly nonequilibrium. When the temperature in the sample center began to increase towards the

fluid jacket temperature, the rate of gas collection declined significantly, and gas production ceased as the temperatures equilibrated with the temperature in the fluid jacket.

The final condition, shown as Image 5 in **Figure 3**, closely resembles the initial condition (Image 1 of **Figure 3**).

### Discussion

The set of experiments described here provides a rich data set for gaining understanding of processes related to hydrate formation and dissociation in a porous medium. Combined use of pressure, temperature, and x-ray CT information enable us to attribute processes to the spatial location where they occur, and not to the bulk of the sample. Our initial conceptual model was that hydrate would form uniformly (but perhaps influenced by the gravitation-induced saturation gradient), the thermal stimulation would cause only dissociation (not formation), the second hydrate formation would be uniform, and dissociation by depressurization would uniformly affect the entire volume. Initially, the hydrate formation was fairly uniform, but occurred preferentially in more porous regions. Thermal dissociation at the outer radius of the sample caused a pressure increase that increased stability in the sample center. Moreover, the second hydrate formation did not occur uniformly, but preferentially in regions not strongly affected by the thermal dissociation. Our dissociation by depressurization was very short lived and affected the bulk of the sample. It was followed by a thermal stimulation in which the temperature gradient was caused by the endothermic hydrate dissociation. Continued evaluation of the data collected, as well as analytical and numerical modeling is under way to enhance our understanding of the processes that occurred.

### Conclusions

Multiple types of measurements are needed to more fully understand processes that occur in formation and dissociation of gas hydrates within porous media. The use of x-ray CT has allowed us to correctly attribute processes to the locations where they occur and not to the bulk system. This work will allow for more accurate parameter estimation through analytic and numerical modeling. Because of the changes that occur during the processes we observed, inverse modeling will likely be needed to best estimate thermal and kinetic parameters from this and similar tests.

**Acknowledgement.** This work was supported by the Assistant Secretary for Fossil Energy, Office of Natural Gas and Petroleum Technology, through the National Energy Technology Laboratory, under the U.S. DOE, Contract No. DE-AC03-76SF00098.

### References

1. Moridis, G. J.; Collett, T. S.; Dallimore, S. R.; Satoh, T.; Hancock, S.; Weatherill, B., Numerical studies of gas production from several CH<sub>4</sub> hydrate zones at the Mallik site, Mackenzie Delta, Canada. *Journal of Petroleum Science and Engineering* **2004**, 43, 219-238.
2. Howe, S. J.; Nanchary, H. R.; Patil, S. L.; Ogbe, D. O.; Chukwu, G. A.; Hunter, R. B.; Wilson, S. J. *Economic analysis and feasibility study of gas production from Alaska North Slope gas hydrate resources*, In Natural Gas Hydrates: Energy Resource Potential and Associated Geologic Hazards,

Vancouver, BC, Canada, 2004; Collett, T.; Johnson, A., Eds. American Association of Petroleum Geologists: Vancouver, BC, Canada, 2004.

3. Kurihara, M.; Ouichi, H.; Masuda, Y.; Narita, H.; Okada, Y. *Assessment of gas productivity of natural methane hydrates using MH21 Reservoir Simulator*, In Natural Gas Hydrates: Energy Resource Potential and Associated Geologic Hazards, Vancouver, BC, Canada, 2004; Collett, T.; Johnson, A., Eds. American Association of Petroleum Geologists: Vancouver, BC, Canada, 2004.

4. Waite, W. F.; Winters, W. J.; Mason, D. H., Methane hydrate formation in partially water-saturated Ottawa sand. *American Mineralogist* **2004**, 89, 1202-1207.